13th World Conference on Earthquake Engineering
Vancouver, B.C., Canada
August 1-6, 2004
Paper No. 3328

ANALYTICAL APPROACH TO THE MEASURED DEFORMATION CHARACTERISTICS OF R/C SHEAR WALLS

Thomas SALONIKIOS[1]

SUMMARY

In this work are presented results from the processing of the measurements that resulted from the experimental testing at the laboratory of eleven Reinforced Concrete walls. The flexural, web shear and sliding shear mechanisms were considered that resist the loads that were imposed at the top of the specimens. The processing of the measurements is related with the estimation of the displacement due to the deformation of the aforementioned individual seismic load resisting mechanisms. Results are presented at comparative envelope – curve diagrams of shear force versus displacement. From the measurements, displacement ductilities are calculated, that resulted from the deformation of all load resisting mechanisms of the specimens and are compared with the displacement ductility that resulted from the deformation of the flexural mechanism of each specimen, with the latest also calculated analytically by considering perfect flexural behavior. From the shape of the envelope curves of the hysteresis loops, result useful conclusions about the contribution of each load resisting mechanism to the inelastic deformations of each specimen and about the changes that were observed to the inelastic deformation due to the parameters variation among the specimens: aspect ratio, existence of axial load, reinforcement quantity and arrangement.

INTRODUCTION

In Reinforced Concrete (R/C) walls, with aspect ratio 1.0 and 1.5, loaded on top with cyclic horizontal load, cracks are formed into all the load resisting mechanisms. The cracks are formed at the two sides of the web, starting from the base and reaching to the upper part of the web. These cracks have an inclination that varies from 0° (at the base) up to 45° (at the web). Due to that cracking, the imposed displacement at top is achieved by partial displacements due to the deformation of flexural, web shear and sliding shear mechanisms (Figure 1). The aforementioned mechanisms resist the imposed deformations. Each one of these mechanisms is composed by secondary mechanisms. The flexural mechanism is composed by the partial mechanisms of tensioned longitudinal reinforcement and the compressed part of the concrete section. The web shear mechanism is composed by the tensioned web reinforcement, by the compressed struts that are defined between diagonal tension cracks at the web and by the tensioned longitudinal

[1] Researcher, Institute of Engineering Seismology & Earthquake Engineering, Thessaloniki, Greece.
Email: salonikios@itsak.gr

reinforcement of the edge column. According the theory of truss mechanism, these individual mechanisms resist the imposed shear at the web of R/C walls.

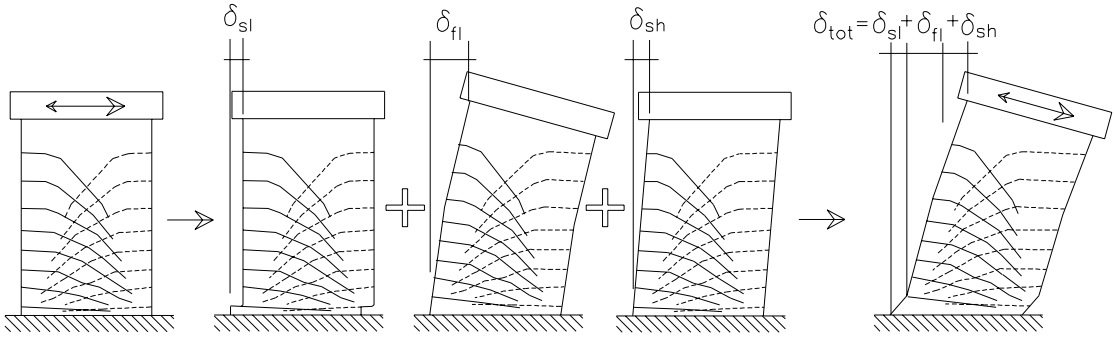

Figure 1. Composition of total displacement from the deformation of each individual seismic load resisting mechanism

The sliding shear mechanism is activated along the flexural cracks at the base of R/C walls and can be considered that is produced from the web shear mechanism by projection to a horizontal level, (Salonikios [1]). The sliding shear mechanism is composed by the dowel action of longitudinal reinforcement, the aggregate interlock and by the concrete friction between the cracks' surfaces. These partial mechanisms compose the main seismic load resisting mechanisms and are taken into account in the case of design and check of a R/C wall according a modern code (e.g. Eurocode 8). In that case the shear force that corresponds to the flexural strength should be lesser than the shear force that corresponds to the failure due to diagonal tension and sliding shear mechanisms. The above code requirements provide to the structure the capacity to exhibit ductile behavior when is subjected to seismic loads higher than the design loads. The plastic hinges formed in this case will be of flexural type. Also measures are taken (through capacity design at beam-column joints) so these flexural plastic hinges will be formed at the ends of beams and at the theoretical clamping level at the base of columns and of R/C walls. The plastic hinge length at the base of R/C walls is a function of the shear ratio (M/Vl). For R/C walls having high shear ratios, edge column's longitudinal reinforcement yields along higher length than for the case of R/C walls of shear ratio 1.0 and 1.5. In the case of such low shear ratios inelastic elongation of flexural reinforcement is concentrated at the base main flexural crack. In this type of plastic hinges (having only one main flexural crack) a combined type of failure appears, as resulted by experiments. In that case, sliding shear failure was observed after the inelastic flexural deformation, for total displacement ductility over 2, (Salonikios [1]).

This work aims to the investigation of the distribution of the deformations to the seismic load resisting mechanisms that are activated within the area of flexural plastic hinges, at the base of R/C walls, with shear ratio 1.0 and 1.5 under low axial loading. Specimens were designed and tested within the framework of elaboration of a PhD thesis at the Aristotle University of Thessaloniki. Results from these tests were presented in details in papers by Salonikios et al. in [1], [2], [3], [4], [5]. In present work from the post processing of the measurements two types of ductilities are calculated. The first type is the displacement ductility due to the deformation of all seismic load resisting mechanisms. The second type is the displacement ductility due to the deformation of flexural mechanism and is estimated by the subtraction, from total displacement at top, of the displacement components due to the shear deformation of the web and the sliding shear deformations along the flexural cracks. Displacement ductility due to the deformation of flexural mechanism is also calculated by the theory of flexure. First curvature ductility is calculated and then by the use of plastic hinge length (Salonikios [5]), the displacement ductility is

calculated, according a relation proposed by other researchers. These calculated ductilities (according theory of flexure) are used for the design of R/C walls. Theoretically calculated ductilities are compared with those estimated from experimental measurements and useful conclusions result.

SHEAR FAILURE AFTER FLEXURAL YIELDING

Within the region of a flexural plastic hinge, a failure of shear mechanisms may appear, after the flexural yielding. This is possible to occur because shear mechanism's resistance is possible to weaken due to the cyclic type of loading and due to high inelastic deformation. It is well known that the moment resisting capacity, of a R/C wall section, increases after yielding. This can be observed at the inelastic branch of strength-deformation diagram of a structural element. The reasons why shear strength is reduced were intensively investigated last years. Views of investigators converge to the point that shear resisting mechanism is weakening due to the reduction of the contribution of the term of concrete friction. This is happening because the shear strength is the sum of the strength of the individual mechanisms of tensile reinforcement and concrete friction (which is reduced due to the cyclic type of loading). By this theory, which has been proved, that applies in R/C columns (Yoshikawa, Miyaki [6], Mander et al. [7]), the case of shear failure, at the web of concrete elements after flexural yielding, is satisfactorily justified.
In the case of flexural yielding, the subject of the estimation of the shear strength along the horizontal cracks at the base remains open. Views converge to the point that along base flexural cracks, during the cycles of loading, re-contact of concrete at the crack's sides can not be developed, resulting thus to shear slip along those cracks. This phenomenon was observed in the case of high inelastic deformation. Open flexural cracks, in both sides of R/C walls, were observed even in cases were an axial load equal with the 10% of the compressive strength of the wall was applied. In that case the mechanism that resists the shear force along the flexural crack is the dowel action. Due to the cyclic type of loading the capacity of longitudinal reinforcement to resist like dowel is also reduced (Salonikios [1], Oesterle et al. [8]).

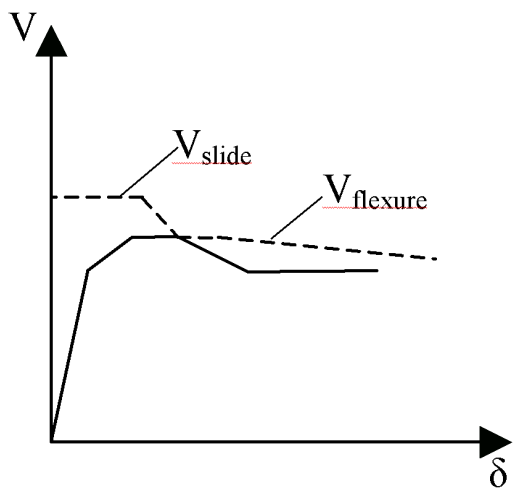

Figure 2. Sliding shear failure after flexural yielding

Above were described two cases according which, after flexural yielding, failure may appear either due to diagonal tension or due to sliding shear (Figure 2). For the R/C walls that are presented in this work, sliding shear deformations after flexural yielding, were measured (especially after total measured displacement ductility 2). From the experimental measurements, the envelope curves of force versus sliding shear displacement, resulted. At the end of the experiments, for the most of specimens, sliding shear displacements were significantly high, indicating thus the weakening of the corresponding

mechanism. At that stage together with the displacement due to the deformation of sliding shear mechanism were recorded displacements due to the deformation of flexural mechanism and web shear mechanism. These components of the total displacements are calculated and presented to the next chapters.

DUCTILITY CAPACITY

The capacity of ductile deformation of R/C walls is satisfactorily described by the ductility factors. For this reason are used the curvature ductility (μ_φ), the rotation ductility (μ_θ) and the displacement ductility (μ_δ) factors, in order to describe the capacity of the section or of the element for inelastic deformation. As was described above, in a R/C wall, subjected to cyclic loading at the top, the imposed displacement is produced by the deformation of all load resisting mechanisms. So for the ratio:

$$\mu_\delta = \frac{\delta_u}{\delta_y} \qquad (1)$$

of the measured quantities, the nominator and the denominator is composed by the sum of the displacements that results from the deformation of individual seismic load resisting mechanisms. So, in every step of loading, the total displacement's ductility is:

$$\mu_{\delta,tot} = \frac{\delta_{fl} + \delta_{sh} + \delta_{sl}}{\delta_y} \qquad (2)$$

where: δ_{fl} : top displacement due to deformation of flexural mechanism
δ_{sh} : top displacement due to deformation of web shear mechanism
δ_{sl} : top displacement due to deformation of sliding shear mechanism

The open subject that arises in that case is the definition of yield displacement δ_y in the relation (2). Even in the case of small imposed displacements as yield displacements, all seismic load resisting mechanisms contribute with deformations, resulting thus to the relation:

$$\delta_y = \delta_{e,fl} + \delta_{e,sh} + \delta_{e,sl} \qquad (3)$$

In the case of experimental measurements, in the diagram of shear strength versus total displacement, the yield displacement can be calculated by one of the known graphical ways (e.g. the method of equivalent areas).

For a R/C wall loaded by a horizontal load at top, the displacement δ_{fl} that result from the deformation of flexural mechanism is estimated by the measurements of purposely located instruments and through simplified calculations. In this case are measured the elongation and the shortening along the confined edge columns. From these measurements, in combination with the shear ratio of the R/C wall, is estimated the top displacement due to the flexural deformation of the wall. For this reason there is a need for measurement of deformation along the confined edge columns of the R/C wall. In this case, the displacement due to the deformation of flexural mechanism (e.g. between points a and b along the axis of a structural element), is given by (Penelis, Kappos [9]):

$$\delta_{fl,ab} = \int_a^b x\,\phi\,dx \qquad (4)$$

Where x is the distance of the infinitesimal length dx from point "a" and "ϕ" is the curvature of the section, which is assumed constant for that length. By this way, the envelope curve of shear force versus displacement due to deformation of flexural mechanism is estimated. The yield point is estimated from this diagram that is plotted discharged from any other displacement.

Top displacement due to the deformation of sliding shear mechanism δ_{sl} along the flexural cracks at specimens' base is directly measured (especially for R/C walls with aspect ratio 1.0 and 1.5 where longitudinal reinforcement yields at the main flexural crack at the base). This measurement is possible by purposely located instrument (LVDT) which measures in direction parallel to the direction of loading.

One side of the instrument is positioned on the specimen (slightly over the area of the main flexural crack) and the other side is located on the anchorage block of the specimen. The definition of yield displacement of sliding shear mechanism is very complicated. It must be emphasised that this sliding shear displacement is not developed, at the specimens' base, as a main failure mechanism, but is developed mostly after the yielding of longitudinal reinforcement of the edge columns of the R/C wall for a total displacement ductility level over 2.

After the estimation of the displacements at the top of the specimens, due to the deformation of the flexural mechanism and the sliding shear mechanism, the displacement due to the web shear deformation, results from the total measured displacements as: $\delta_{sh}=\delta_{tot}-\delta_{fl}-\delta_{sl}$. Alternatively the displacement at the top of the specimens due to the web shear deformation is possible to be estimated, from the measurements, by considering the matrix of deformation of plane disk, as was described in work Salonikios [1].

SHAPE OF ENVELOPE CURVES OF RESISTING MECHANISMS

According the suggested methodology, after the test of a cantilever structural element that is loaded by a horizontal force at the top, the diagrams of measured quantities (e.g. V-δ_{tot}) or of the quantities that result from the analytical processing of the experimental measurements (e.g. V-δ_{fl}, V-δ_{sh}, V-δ_{sl}) can be drawn. By considering the shape of these diagrams, useful conclusions result on the response of the specimens, especially in the case of combined type of failure. In case of yielding and afterwards of inelastic deformation of a mechanism, it is obvious that the shape of load - displacement curve will be defined by the behavior laws of that mechanism that fails. In this case the open subject is what will be the shapes of the load – displacement curves of the mechanisms that do not fail. In cases that there is not interaction among seismic load resisting mechanisms the answer is obvious. The envelope curves diagrams for the mechanisms that do not fail will have the strength that corresponds to the strength of the mechanism that is deformed inelastically (fails). The displacement of the envelope curves of the mechanisms that are not deformed considerably after yielding, is reduced after the reduction of strength. For the specimens of the present work did not appear yielding to the web shear mechanism. For the hysteresis loops of this mechanism, reduction of the displacement is observed (due to shear deformation at the web), after the reduction of the strength (due to cyclic loading) of the mechanism that is deformed inelastically.

Conversely, in structural elements where is not significant which mechanism fails, useful conclusions can be drawn from the observation of the shape of the envelope curves of shear force versus the displacement of each individual seismic load resisting mechanism. Thus, can be concluded which mechanism yielded, at which mechanism inelastic deformations were developed and which mechanism(s) failed at the end of the experiment. The possible shapes of the envelope curves that may result from the deformation of each individual seismic load resisting mechanism are drawn in figure 3 and are explained below.

A) Ascending inclination initially, ascending inclination with smaller slope afterwards and reduction of the strength and displacement at the last cycles.

B) Ascending inclination initially, ascending inclination with smaller slope afterwards, then almost horizontal inclination and reduction of the strength and displacement at the last cycles.

C) Ascending inclination initially, ascending inclination with smaller slope afterwards, then almost horizontal inclination, reduction of the strength and increase of the displacement at the last cycles.

In case (A) it is significant that cracks are formed in the mechanism that is represented, while reinforcement (of the mechanism to whom the diagram is related) does not yield. In case (B) cracks are formed in the mechanism that is represented and following yielding and inelastic deformation are observed. Due to the reduction of displacement at the last cycles, failure occurs to other mechanism. In case (C), it is obvious that a mechanism is described which yields, is deformed inelastically and finally fails. Case (C) is possible to be observed in two mechanisms simultaneously. This fact indicates that final failure occurs in these two mechanisms.

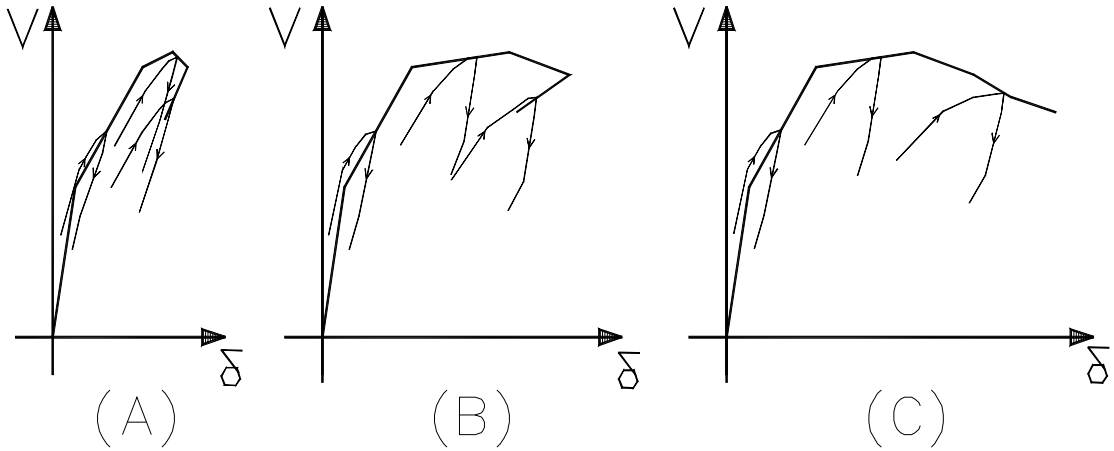

Figure 3. Possible shapes of the envelope curves for the individual seismic load resisting mechanisms

Envelope curves of type (C), are observed in most specimens, related with this work, for the flexural and sliding shear resisting mechanisms simultaneously. For all specimens the envelope curves of the web shear mechanism are of type (A). These diagrams are presented in detail at the following chapters.

EXPERIMENTAL RESULTS

Specimens

Experimental and analytical results that are presented in this work resulted from tests at the laboratory of Concrete Structures of Aristotle University of Thessaloniki, Greece. Eleven reinforced concrete shear wall specimens have been tested. The construction scale was 1:2.5. Rectangular cross-section dimensions were 1200×100(mm), the height of the LSW group of specimens was 1200(mm) and for the MSW group of specimens was 1800(mm). The five LSW specimens had an aspect ratio equal to 1.0 (LSW1-LSW5) and the six MSW specimens had an aspect ratio equal to 1.5 (MSW1-MSW6). At the confined edge columns Ø8 steel bars were used as longitudinal reinforcement and Ø4.2 steel bars as confinement reinforcement. Specimens LSW1, MSW1, MSW6 had 8Ø8 longitudinal steel bars per edge column. For the rest of the specimens this reinforcement was 6Ø8. Specimens LSW4 and MSW4 had three unconfined diagonal bars ($\Phi=\pm45^{o}$), along each direction, which passed through the middle of their cross-section at the base. Specimens LSW5 and MSW5 had also three diagonal steel bars in each direction that passed through the confined edge columns at the specimens base. On the web of every specimen a double grid of Ø4.2/10 was located, except for the LSW1, MSW1 and MSW6 specimens which had additionally an extra single grid of Ø8/17. At the base of specimen MSW6 the reinforcement was connected by lap splicing, without concrete roughening and additional reinforcement (Figure 4). Specimens were loaded by top displacement cycles until a 25% drop of the maximum strength was observed. The typical displacement history consisted of three initial single cycles at ±2, ±4, ±6 mm, followed by three cycles, at the same amplitude, with increments of 2mm up to a displacement of 16mm, and increments of 4mm thereafter, up to the failure point. Specimens LSW3 and MSW3 were also subjected to axial loading equal to 7% of the compressive strength of the R/C walls (165kN). At the top of the specimens a R/C stiff beam was constructed where a horizontal actuator was tied in order to apply horizontal load and a vertical actuator was seated in order to apply axial loading. At the base of the specimens there was a R/C beam for the anchorage of longitudinal reinforcement and for the anchoring of the specimens at the 1m thickness laboratory's floor.

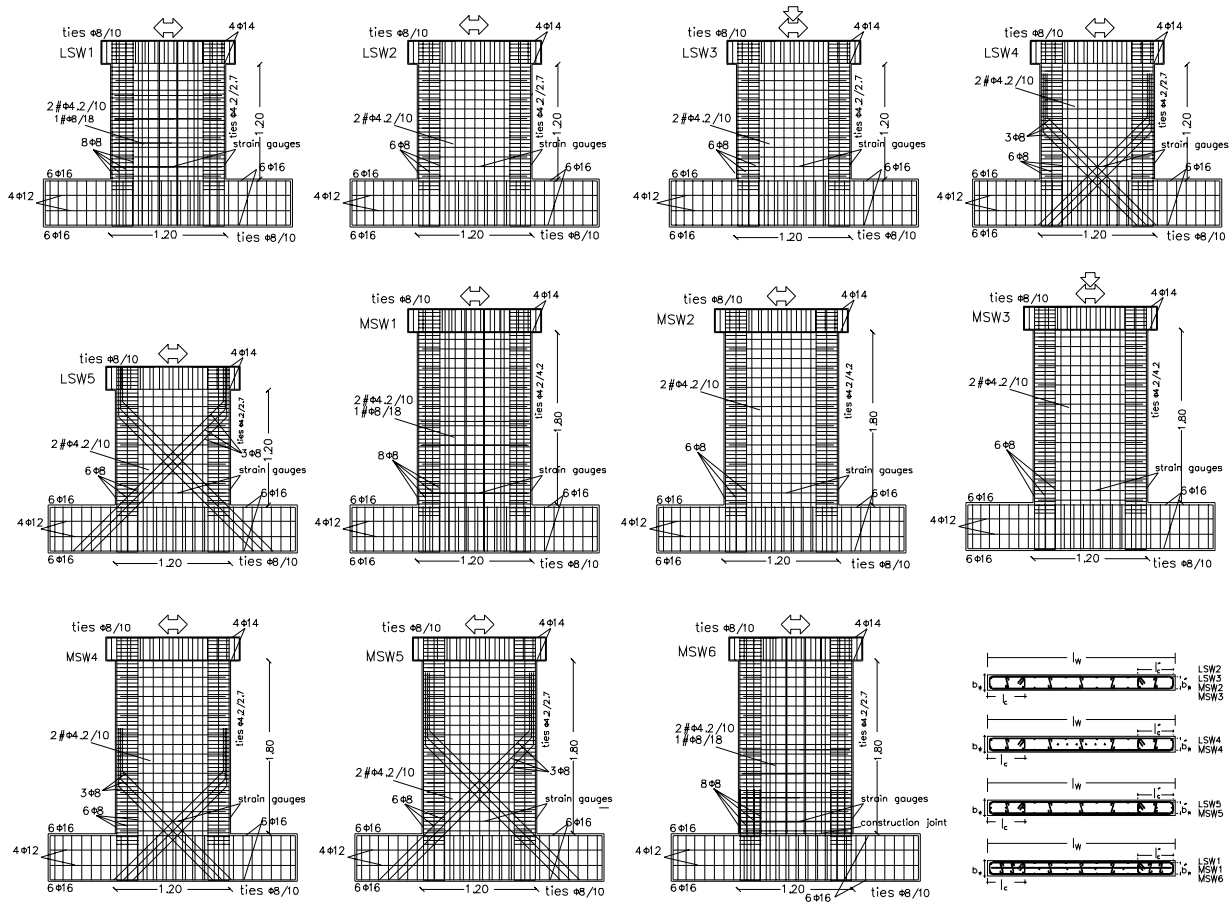

Figure 4. Reinforcement layout in wall specimens

Envelope curves of resisting mechanisms

After the tests and the processing of the measurements, the envelope curves of the hysteresis loops resulted, for each individual seismic load resisting mechanism. The methodology that was used was described at the chapter with the title Ductility Capacity. In the left column are presented for each specimen the envelope curves that correspond to the behavior of sliding shear (V-δ_{sl}), of web shear (V-δ_{sh}), and of flexural (V-δ_{fl}) mechanisms. In the right column are presented, for each specimen, the hysteresis loops' envelope curves that result from the sum of the displacements due to the deformations of seismic load resisting mechanisms: V-δ_{sl} ,V-δ_{sl+sh}, V-$\delta_{sl+sh+fl}$ (Figures 5,6,7). From the observation of the shape of the envelope curves results the conclusion that, during loading, the flexural and sliding shear mechanisms, yield, are deformed inelastically and finally fail (case C). In case of specimens LSW1 and LSW2, limited inelastic deformation of the flexural mechanism is observed, since after the reduction of the strength, reduction of the displacement is observed as well (case B). For all other specimens combined type of failure (flexural and sliding shear) is observed. The web shear mechanism does not yield in any specimen, since, in every case, after the reduction of the strength of the specimens, reduction of the displacements, due to the deformation of that mechanism, is observed too (case A). The resulting shear displacements have low values (mean value 1.7mm) indicating thus that there is probably an accuracy problem. From the fact that similar behavior is observed in all specimens, results the conclusion that the presented envelope curves are real.

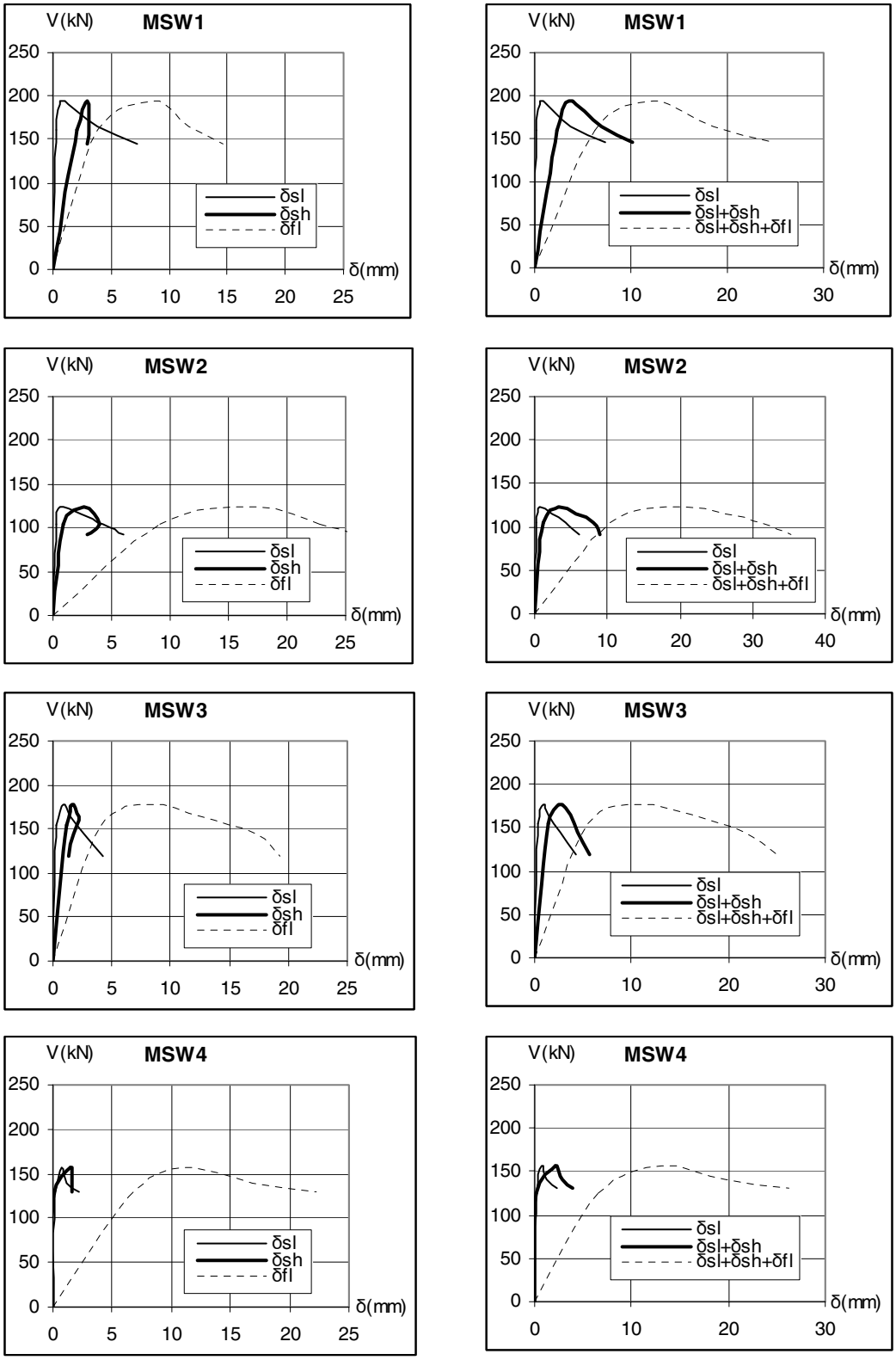

Figure 5. Hysteresis loops' envelop curves as resulted from the experimental measurements (specimens MSW1 – MSW4)

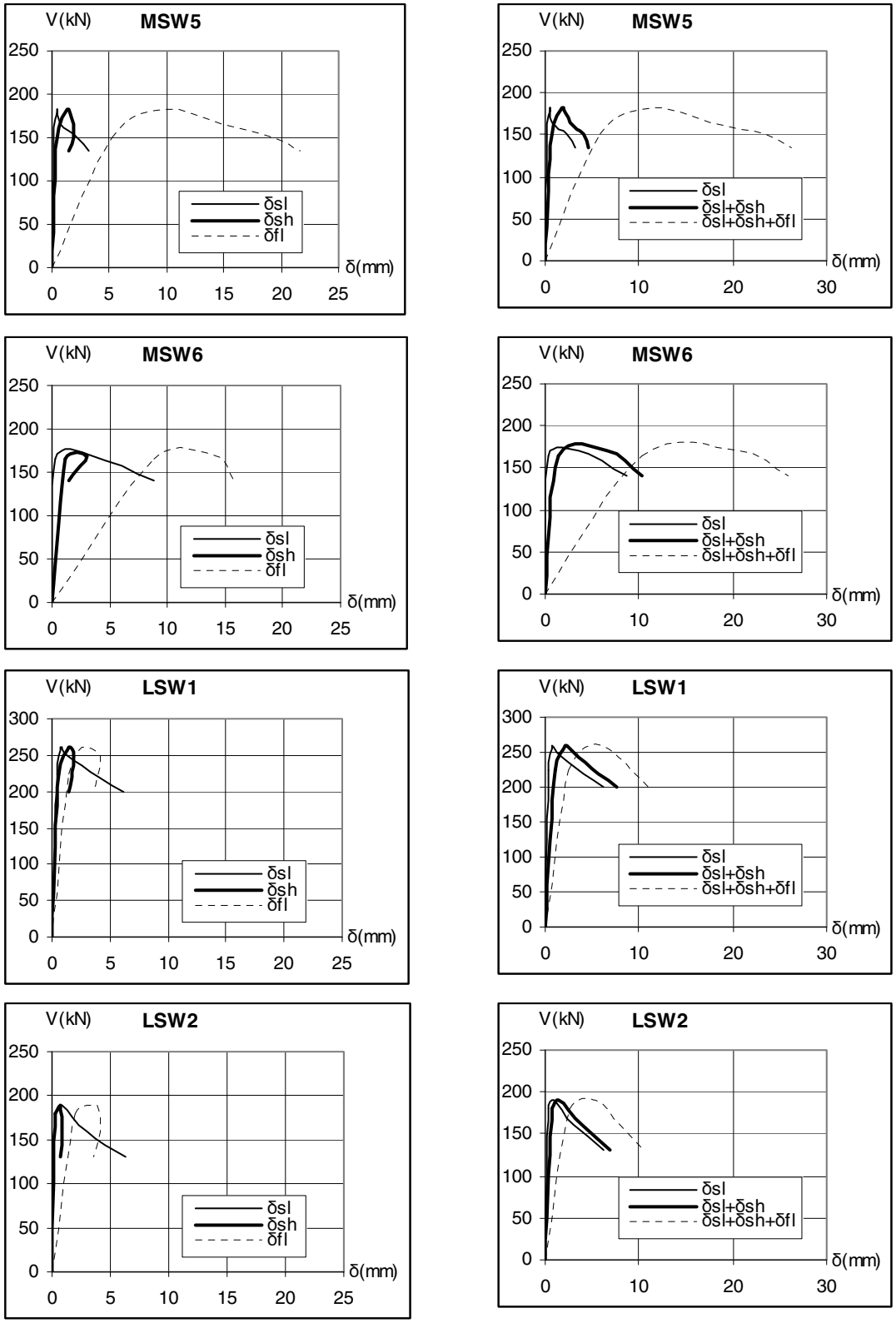

Figure 6. Hysteresis loops' envelop curves as resulted from the experimental measurements (specimens MSW5, MSW6, LSW1, LSW2)

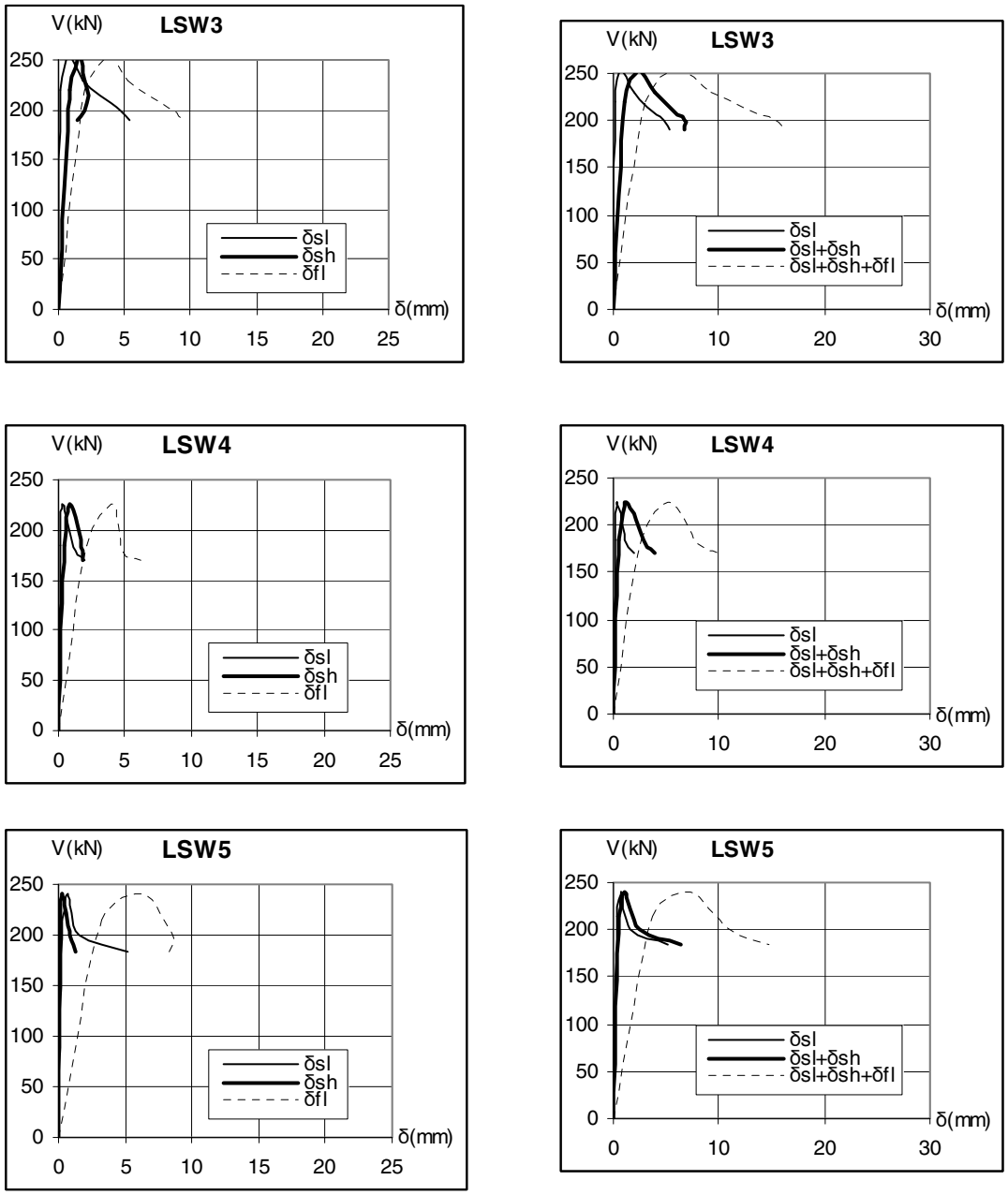

Figure 7. Hysteresis loops' envelop curves as resulted from the experimental measurements (specimens LSW3 – LSW5)

Ductility calculations

From the aforementioned diagrams the ductilities are calculated that result from the consideration of total displacements ($\mu_{\delta,tot}$) and of the displacements at the top of the specimens, that correspond to the deformation of flexural mechanism ($\mu_{\delta,fl}$). Total displacements were recorded at the top of the specimens during the experiment. Displacement ductility of flexural mechanism is calculated from the displacements that correspond to the deformation of flexural mechanism and resulted from the processing of experimental measurements. At the table that follows are presented the aforementioned ductilities (Table 1).

Table 1. Total displacements' ductility and displacements' ductility from the deformation of flexural mechanism, as resulted from experimental measurements

Duct.	MSW1	MSW2	MSW3	MSW4	MSW5	MSW6	LSW1	LSW2	LSW3	LSW4	LSW5
$\mu_{\delta,tot}$	4.0	3.4	4.6	4.0	4.5	2.5	4.6	3.9	5.3	3.8	4.0
$\mu_{\delta,fl}$	3.8	2.9	4.9	3.5	4.2	1.8	2.4	1.8	4.7	3.0	2.5

As it is concluded from table 1, total displacement ductilities are higher than the displacement ductilities due to the deformation of flexural mechanism. The question that arises in this case is which ductility should be used for the calculation of total ductility of a building or a bridge that these R/C walls are part of. This question arises even in the case where the behavior factor of such structure should be estimated, for the calculation of seismic loads. For such calculations, the total displacement ductility is used. In this case the behavior factor results higher than in the case of use of the displacement ductilities due to the deformation of flexural mechanism. Due to the low shear ratio of the walls (1.0, 1.5) the structure to which these elements belong, should have low period of vibration. For this reason the differences to the behavior factors that are estimated by the use of $\mu_{\delta,tot}$ or $\mu_{\delta,fl}$ should be small. Obviously the value of the behavior factor is influenced by other parameters as the inclination of the strength – deformation envelope curve after yield, the inclination of the descending branch of this curve, the reduction of inclination of the reloading curve of the hysteresis loops and the pinching of the hysteresis loops at the region of the origin of the axes of load – displacement diagram. These parameters will be considered in future publications so in the present study are ignored.

ANALYTICAL RESULTS

Reinforced concrete walls designed according modern codes, like these of the present work, are expected to exhibit mainly flexural behavior. By assuming such behavior, in the following the curvature ductility is calculated by the use of appropriate program and the corresponding displacement ductility is calculated by the use of a proposed formula.

Curvature ductility

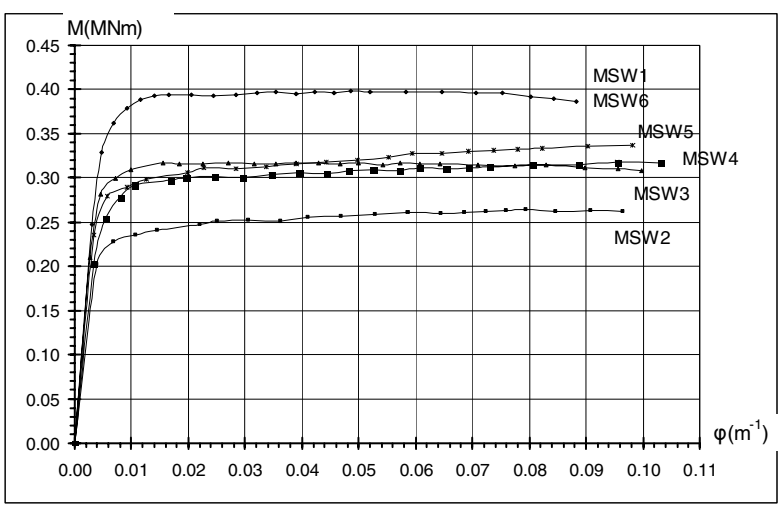

Figure 8. M-ϕ diagrams for MSW group of specimens, as resulted by the R.C.COL.A program

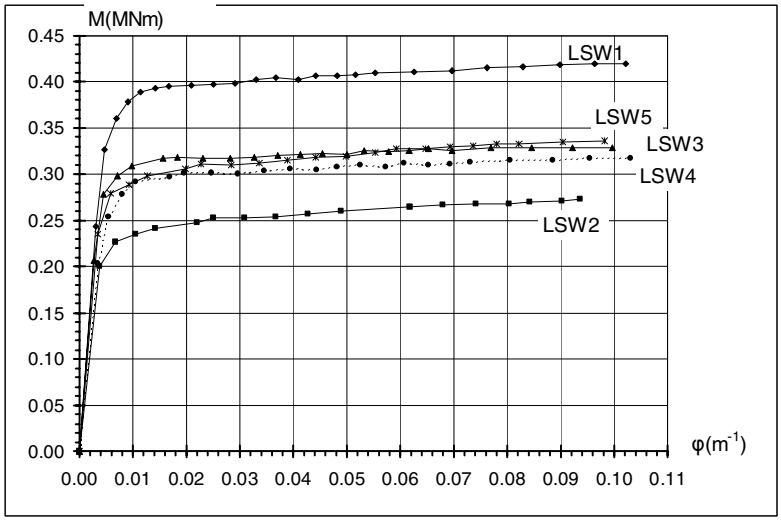

Figure 9. M-ϕ diagrams for LSW group of specimens, as resulted by the R.C.COL.A program

For the calculation of curvature ductility of the specimens, the fiber model is used. The cross-section of the R/C walls is divided into fibers where the materials' laws (confined concrete, unconfined concrete, reinforcement) are also modeled. Through a repeat process, the moment carrying capacity (M) corresponding to various values of the curvature of the section (ϕ) are calculated. The software that is used for this purpose is the R.C.COL.A program. The resulted M-ϕ diagrams are presented in figures 8 and 9. The curvature ductility for each specimen is presented at the table that follows (Table 2).

Table 2. Curvature ductilities as resulted from the analysis

Duct.	MSW1	MSW2	MSW3	MSW4	MSW5	MSW6	LSW1	LSW2	LSW3	LSW4	LSW5
μ_φ	14.0	14.2	19.5	14.7	14.4	14.0	15.0	14.2	16.6	14.7	15.8

Displacement ductility

The displacement ductility for each specimen is calculated from the curvature ductility, by the use of the following relation (5) that was proposed by Paulay, Priestley [10]:

$$\mu_\delta = 1 + 3(\mu_\phi - 1)\frac{\ell_p}{\ell}(1 - 0.5\frac{\ell_p}{\ell}) \qquad (5)$$

The plastic hinge length that should be considered, for the R/C walls of the present study (aspect ratio 1.5 and 1.0), was estimated through a parametric study (Salonikios [5]) and is given by the following relation (6):

$$\ell_p = 0.044h_w + 0.014d_b f_y \qquad (6)$$

In Eq.(6), h_w is the height at which bending moments have zero value (considering triangle moment diagram in case of cantilever R/C walls), d_b is the diameter of edge column's longitudinal reinforcement and f_y is the yield stress of that reinforcement. For walls investigated herein, plastic hinge length for MSW series of specimens according Eq.(6) is L_p=0.145m while for LSW series of specimens the corresponding length is L_p=0.119m. By the use of these data and for the curvature ductilities that were calculated in previous paragraph, by the use of R.C.COL.A. program, the displacement ductilities of the R/C walls according relation (5) result as shown in table 3:

Table 3. Displacement ductility as resulted according equation (5)

Duct.	MSW1	MSW2	MSW3	MSW4	MSW5	MSW6	LSW1	LSW2	LSW3	LSW4	LSW5
$\mu_{\delta,fl}$	4.0	4.1	5.3	4.2	4.1	4.0	5.0	4.7	5.4	4.9	5.2

From the comparison of displacement ductility, due to the deformation of flexural mechanism ($\mu_{\delta,fl}$) in R/C structural walls, that was estimated from the processing of the experimental measurements (table 1) and from analytical calculations (table 3) results the conclusion that these values are quite different. The observed differences are due to the ignorance of shear deformations in relation (5).

CONCLUSIONS

Results were presented from the processing of the measurements, which were recorded during the testing at the laboratory, of eleven R/C structural wall specimens. The hysteresis loop envelope curves are presented, that describe the load – deformation behaviour of the three individual mechanisms that are deformed when a horizontal load is applied at the top of the specimens. Possible types of envelope curves, that were expected to result, are presented at the diagrams A, B, C of figure 2. All these three types were observed at the diagrams of envelope curves. Main conclusions are that web shear mechanism did not yielded in any specimen (behavior type A). In all specimens were recorded top displacements due to the deformation of sliding shear mechanism. In specimens MSW4, MSW5, LSW4, LSW5 which had diagonal reinforcement and specimens MSW3 and LSW3 which were loaded by compressive axial force, these displacement were significantly reduced. From the observation of the envelope curves results the conclusion that flexural mechanism yields initially and is deformed inelasticaly afterwards. While the inelastic flexural deformation increases, for total displacement ductility over two, the displacement due to the deformation of sliding shear mechanism was significantly increased, indicating thus the weakening of this mechanism. Finally failure occurred at both flexural and sliding shear mechanisms. In specimens LSW1 and LSW2, inelastic deformation of the flexural mechanism was limited (behavior type B).

From the process of the experimental measurements resulted that the displacement ductility, due to the deformation of all seismic load resisting mechanisms ($\mu_{\delta,tot}$), is higher than the displacement ductility due to the deformation of the flexural mechanism ($\mu_{\delta,fl}$). From the analytical calculation of the curvature ductility resulted the displacement ductility by considering perfect flexural behaviour. The analytically resulted displacement ductility was higher than the corresponding ductility due to the deformation of flexural mechanism that resulted from the experimental measurements. Difference between analytically estimated ductility ($\mu_{\delta,fl}$) and the ductility that was estimated from experimental measurements ($\mu_{\delta,tot}$) was lower. For the specimen MSW6 where the reinforcement was connected by lap splicing, without concrete roughening and additional reinforcement, the experimentally measured ductilities due to the deformation of all strength-resisting mechanisms and due to the deformation of flexural mechanism were much lower than the analytically calculated flexural displacement ductility. For this reason, the provisions of codes that discourage the connection of steel bars by lap splicing, at the regions where plastic hinge formation is expected, are proved reasonable.

The modelling of the sliding shear mechanism's behaviour, that appears after flexural yielding, needs more research effort in order to form accurate and reliable models. This modelling is more complicated if will be considered that, at every step of loading, all load resisting mechanisms are deformed.

REFERENCES

1. Salonikios T. N. "Shear strength and deformation patterns of R/C walls with aspect ratio 1.0 and 1.5 designed to Eurocode 8". Engineering Structures Journal 2002; 24(1): 39-49.

2. Salonikios T. N., Kappos A. J., Tegos I. A., and Penelis G. G. "Cyclic load behavior of low-slenderness RC walls: Design basis and test results". ACI Structural Journal 1999; 96(4): 649-60.

3. Salonikios T. N., Kappos A. J., Tegos I. A., and Penelis G. G. "Cyclic load behavior of low-slenderness RC walls: Failure modes, strength and deformation analysis, and design implications". ACI Structural Journal 2000; 97(1): 132-41.

4. Salonikios T. N. "Side column axial deformations of cyclic loaded R/C walls with aspect ratio 1.0 & 1.5". Proceedings of the 12th European Conference on Earthquake Engineering, London, UK. Paper no. 34. Elsevier Science, 2002.

5. Salonikios T. N. "Deformation characteristics of R/C walls, with low aspect ratio, subjected to cyclic loads". Proceedings of the FIB Symposium on Concrete Structures in Seismic Regions, Athens, Greece. Paper no. 200. Technical Chamber of Greece, 2003.

6. Yoshikawa H., Miyagi T. "Ductility and Failure Modes of Single Reinforced Concrete Columns". P. Benson Shing, Tada-aki Tanabe, Editors. Modelling of inelastic behaviour of RC structures under seismic loads. ASCE, 2001:351-68.

7. Mander J., Kim J. H., Dutta A. "Shear-Flexure Interaction Seismic Analysis and Design". P. Benson Shing, Tada-aki Tanabe, Editors. Modelling of inelastic behaviour of RC structures under seismic loads. ASCE, 2001:369-83.

8. Oesterle R. G., Fiorato A. E., Aristizabal – Ochoa J. D. and Corley W. G. "Hysteretic Response of Reinforced Concrete Structural Walls". ACI SP-63. Reinforced Concrete Structures Subjected to Wind and Earthquake Forces. ACI, Detroit, Mich., 1980: 243-73

9. Penelis G.G. and Kappos, A.J. "Earthquake-resistant concrete structures". E & FN SPON (Chapman & Hall), London, UK, 1997.

10. Paulay T., Priestley M. J. N. "Seismic design of reinforced concrete and masonry buildings". John Wiley & Sons, USA, 1992.